PANACM 2015
1st Pan-American Congress on Computational Mechanics

In conjunction with the XI Argentine Congress on Computational Mechanics, MECOM 2015

27-29 April, 2015, Buenos Aires, Argentina

1st Pan-American Congress on Computational Mechanics - PANACM 2015

XI Argentine Congress on Computational Mechanics - MECOM 2015

Proceedings of the

1st Pan-American Congress on Computational Mechanics

and

XI Argentine Congress on Computational Mechanics

held in Buenos Aires, Argentina
27-29 April 2015

Edited by:

Sergio R. Idelsohn (Chairman)
International Centre for Numerical Methods in Engineering (CIMNE) - Catalan Institute for Research and Advanced Studies (ICREA), Barcelona, Spain
Centro de Investigaciones de Métodos Computacionales (CIMEC), Santa Fe, Argentina

Victorio Sonzogni
Centro de Investigaciones de Métodos Computacionales (CIMEC), Santa Fe, Argentina

Alvaro Coutinho
High Performance Computing Center (COPPE)
Federal University of Rio de Janeiro, Brazil

Marcela Cruchaga
Universidad de Santiago de Chile, Chile

Adrian Lew
Stanford University, Stanford (California), USA

Miguel Cerrolaza
Instituto Nacional de Bioingeniería de la Universidad Central de Venezuela
Caracas, Venezuela

A publication of:

International Center for Numerical Methods in Engineering (CIMNE)
Barcelona, Spain

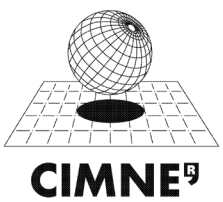

1st Pan-American Congress on Computational Mechanics

and

XI Argentine Congress on Computational Mechanics

First edition, April 2015

Printed by: Artes Gráficas Torres S.L., Huelva 9, 08940 Cornellà de Llobregat, Spain

E-book:
ISBN: 978-84-943928-2-5

PREFACE

This volume contains the Proceedings of the the First Pan-American Congress on Computational Mechanics, **PANACM 2015** and the XI Argentine Congress on Computational Mechanics, **MECOM 2015**, held in Buenos Aires, Argentine, April 27–29, 2015.

PANACM 2015 is the first conference organized under the auspices of the International Association for Computational Mechanics (IACM) to promote the Computational Mechanics in the Americas as a one region.

The purpose of PANACM series is to promote achievements by encouraging young researchers, stimulating education in universities, disseminating modern trends in the field amongst scientists and engineering and mainly, facilitating the interchange of knowledge between the North and the South.

The main objective of PANACM 2015 is to become a forum for state of the art presentations and discussions of mathematical models, numerical methods and computational techniques for solving problems of multidisciplinary character in science and engineering. The conference goal is to make a step forward in the formulation and solution of real life problems with a multidisciplinary nature and industrial interest, accounting for all the complex mathematical models involved in the physical description of the problem.

PANACM 2015 is organized in conjunction with the XI Argentine Congress on Computational Mechanics, MECOM 2015, a traditional and very well known congress in the Argentinean science community.

PANACM 2015, together with MECOM 2015, has attracted around 600 participants, coming from all over the world. All together some 540 lectures will be presented, including 8 Plenary lectures, 12 Semi-Plenary lectures and 43 Keynote Lecturers, which reflect the current state of the research and advances in engineering practice in the Computational Mechanics science.

The International Centre for Numerical Methods in Engineering (CIMNE) organizes this Conference jointly with the Asociación Argentina de Mecánica Computacional (AMCA). The organizers acknowledge the encouragement and support of CIMNE and AMCA and the special interest of the IACM, under whose auspices this conference is held.

All accepted abstracts can be found online on the website of PANACM 2015: http://congress.cimne.com/panacm2015/frontal/ProgIntro.asp. Submitted full papers have been published in an e-book (ISSB: 978-84-943928-2-5), also available on the website: http://congress.cimne.com/panacm2015/frontal/doc/EbookPANACM2015.pdf.

The organizers would like to thank the authors for submitting their contributions and for their respect of the deadlines. Special thanks go to the colleagues who contributed to the organization of the 45 Mini-Symposia to be presented during the Congress.

Sergio Idelsohn (Chairman)	Victorio Sonzogni (Argentina)	Alvaro Coutinho (Brazil)	Marcela Cruchaga (Chile)	Adrian Lew (USA)	Miguel Cerrolaza (Venezuela)

1st Pan-American Congress on Computational Mechanics – PANACM 2015
XI Argentine Congress on Computational Mechanics – MECOM 2015
S. Idelsohn, V. Sonzogni, A. Coutinho, M. Cruchaga, A. Lew & M. Cerrolaza (Eds)

COMPARATIVE ANALYSIS OF NEW SHEAR LOCKING-FREE FINITE ELEMENT WITH OTHER COMMONLY USED APPROACHES IN VIBRATION ANALYSIS OF MINDLIN PLATES

I. SENJANOVIĆ[1], N. VLADIMIR[1], D.S. CHO[2], M. JOKIĆ[1], T.M. CHOI[3]

[1]University of Zagreb, Faculty of Mechanical Engineering and Naval Architecture
Ivana Lucica 5, 10000 Zagreb, Croatia
nikola.vladimir@fsb.hr, www.fsb.unizg.hr

[2]Pusan National University, Department of Naval Architecture and Ocean Engineering
63 beon-gil 2, Busandaehak-ro, Geumjeong-gu, Busan, 609-735, Korea

[3]Createch Co., Ltd.
Room 1312, Centum IS tower, 1209 Jaesong-dong, Haeundae-gu, Busan, 612-050, Korea

Key words: Mindlin Plate Theory, Shear Locking, Vibration, FEM.

Abstract. This paper is dedicated to validation of newly developed shear locking-free finite element (FE) for the vibration analysis of Mindlin plates. First, the state-of-the art in thick plate vibration theories and analysis methods is described and basic equations of the original and advanced Mindlin plate theories, respectively, are listed. Then, a detailed description of shear-locking free rectangular finite element is provided. Bending deflection is used as a potential function for the definition of total (bending and shear) deflection and angles of cross-section rotations. Extensive calculations are done by using developed in-house codes and standard commercial FE tools. Also, comparisons with analytical solutions and energy-based assumed mode method results are included. In addition, convergence of the developed finite element is checked. Natural vibration analyses of rectangular plates having different edge constraints, utilizing the proposed quadrilateral FE, show very good agreement with other commonly used methods.

1 INTRODUCTION

Thick plates are primary constitutive members in many engineering structures. They can be used as engine foundations, elements of reinforced concrete bridges or parts of different floating structures, etc. The thick plate theory represents an issue for very long time, i.e. from the first works published by Reissner and Mindlin [1,2]. As can be seen in the literature survey presented by Liew et al. [3], many concepts for the vibration analysis of thick plates, based both on analytical and numerical solution of equilibrium equations, have been worked out. There are different analytical methods differing on which functions are kept as fundamental ones in the reduction of the system of differential equations of motion [4]. However, analytical solutions are applicable only to simply supported plates or plates with two opposite edges simply supported. For plates with arbitrary edge constraints, including also elastically restrained edges, different variants of the Rayleigh-Ritz (energy) method are on disposal. Their accuracy is dependent on

the chosen set of orthogonal functions for the assumed natural modes, where two dimensional polynomials or static Timoshenko beam deflection functions, [5] and [6,7,8,9], respectively, can be used. Nowadays, FEM represents advanced and widespread numerical tool in structural engineering. It can be applied to vibration analysis of thick plates of any shape including all possible sets of boundary conditions. However, shear locking problem associated with finite elements can appear. Namely, in the Mindlin thick plate theory shear deformations are taken into account, and application of ordinary low-order finite element is not capable to reproduce the pure bending modes in the limit case of thin plate. This shear locking problem arises due to inadequate dependence among transverse deflection and two rotations. Usually, the developed finite elements are based on direct application of the Mindlin plate theory, which deals with plate deflection and angles of rotation as three basic variables. Although, there are different methods for shear locking elimination, it seems to be more reasonable to avoid its appearance implicitly.

This paper outlines a new procedure for determining properties of thick plate finite elements, based on the modified Mindlin theory for moderately thick plate. Bending deflection is used as a potential function for the definition of total (bending and shear) deflection and angles of cross-section rotations [4,10]. As a result of the introduced interdependence among displacements, the shear locking problem, present and solved in known finite element formulations, is implicitly avoided [11,12]. Based on the developed theoretical model, in-house code has been developed and applied to vibration analyses of rectangular plates with different thickness to length (width) ratios and different sets of boundary conditions. Since the special attention is paid to the validation of newly introduced finite element, comparisons are made to the results available in the relevant literature, analytical solutions [4,10], solutions obtained by the assumed mode method [8] as well as to those obtained by general purpose finite element software [13,14]. In addition, convergence study is performed and shows superiority of the developed FE in the case of thin and moderately thick plate.

2 FUNDAMENTALS OF THE ORIGINAL AND ADVANCED MINDLIN THEORIES

The Mindlin theory deals with three general displacements, i.e. plate deflection w, and angles of cross-section rotation about y and x axis, ψ_x and ψ_y, respectively. The following relations between sectional forces, i.e. bending moments, M_x and M_y, torsional moments, M_{xy} and M_{yx}, and transverse shear forces, Q_x and Q_y, and displacements via deformations are specified, [1,2]

$$M_x = D\left(\frac{\partial \psi_x}{\partial x} + \nu \frac{\partial \psi_y}{\partial y}\right), \qquad M_y = D\left(\frac{\partial \psi_y}{\partial y} + \nu \frac{\partial \psi_x}{\partial x}\right), \quad M_{xy} = M_{yx} = \frac{1}{2}(1-\nu) D\left(\frac{\partial \psi_x}{\partial y} + \frac{\partial \psi_y}{\partial x}\right),$$
$$Q_x = S\left(\frac{\partial w}{\partial x} + \psi_x\right), \quad Q_y = S\left(\frac{\partial w}{\partial y} + \psi_y\right), \tag{1}$$

where

$$D = \frac{Eh^3}{12\left(1-\nu^2\right)}, \qquad S = kGh, \tag{2}$$

is plate flexural rigidity and shear rigidity, respectively, h is plate thickness, k is shear coefficient, E and $G = E/\left(2\left(1+\nu\right)\right)$ are Young's and shear modulus, respectively, while ν is Poisson's ratio.

The plate is loaded with transverse inertia load and distributed inertia moments

$$q = -\bar{m}\frac{\partial^2 w}{\partial t^2}, \qquad m_x = J\frac{\partial^2 \psi_x}{\partial t^2}, \qquad m_y = J\frac{\partial^2 \psi_y}{\partial t^2} \tag{3}$$

where $\bar{m} = \rho h$ and $J = \rho h^3/12$ are plate specific mass per unit area and its moment of inertia, respectively, and ρ is mass density. Equilibrium of sectional and inertia forces, i.e. moment about y and x axis and transverse forces read

$$\frac{\partial M_x}{\partial x} + \frac{\partial M_{xy}}{\partial y} - Q_x = m_x, \qquad \frac{\partial M_y}{\partial y} + \frac{\partial M_{yx}}{\partial x} - Q_y = m_y, \qquad \frac{\partial Q_x}{\partial x} + \frac{\partial Q_y}{\partial y} = -q. \tag{4}$$

By substituting Eqs. (1) and (3) into (4) one arrives at three differential equations of motion (well-known Mindlin equations)

$$\frac{D}{S}\left[\frac{\partial^2 \psi_x}{\partial x^2} + \frac{1}{2}\left(1-\nu\right)\frac{\partial^2 \psi_x}{\partial y^2} + \frac{1}{2}\left(1+\nu\right)\frac{\partial^2 \psi_y}{\partial x \partial y}\right] - \left(\frac{\partial w}{\partial x} + \psi_x\right) - \frac{J}{S}\frac{\partial^2 \psi_x}{\partial t^2} = 0, \tag{5}$$

$$\frac{D}{S}\left[\frac{\partial^2 \psi_y}{\partial y^2} + \frac{1}{2}\left(1-\nu\right)\frac{\partial^2 \psi_y}{\partial x^2} + \frac{1}{2}\left(1+\nu\right)\frac{\partial^2 \psi_x}{\partial x \partial y}\right] - \left(\frac{\partial w}{\partial y} + \psi_y\right) - \frac{J}{S}\frac{\partial^2 \psi_y}{\partial t^2} = 0, \tag{6}$$

$$\Delta w + \frac{\partial \psi_x}{\partial x} + \frac{\partial \psi_y}{\partial y} - \frac{\bar{m}}{S}\frac{\partial^2 w}{\partial t^2} = 0, \tag{7}$$

where $\Delta(.) = \frac{\partial^2(.)}{\partial x^2} + \frac{\partial^2(.)}{\partial y^2}$ is the Laplace differential operator.

According to the advanced vibration theory of moderately thick plate [10] deflection of plate consists of beam deflection and shear contribution as in Timoshenko beam theory [15], Fig. 1

$$w(x,y,t) = w_b(x,y,t) + w_s(x,y,t). \tag{8}$$

It is also specified that only bending deflection causes the rotation of plate cross-section, Fig. 1

$$\psi_x = -\frac{\partial w_b}{\partial x}, \qquad \psi_y = -\frac{\partial w_b}{\partial y}. \tag{9}$$

Moreover, according to advanced vibration theory of moderately thick plate [4], system of three differential equations (5), (6) and (7), respectively, can be reduced to only one with the unknown bending deflection

$$D\Delta\Delta w_b - J\left(1 + \frac{\bar{m}D}{JS}\right)\frac{\partial^2}{\partial t^2}\Delta w_b + \bar{m}\frac{\partial^2}{\partial t^2}\left(w_b + \frac{J}{S}\frac{\partial^2 w_b}{\partial t^2}\right) = 0 \tag{10}$$

The bending deflection is a potential function since the remaining displacements w_s, ψ_x and ψ_y can be expressed by its derivatives. Once w_b is determined, the total deflection reads

$$w = w_b + \frac{J}{S}\frac{\partial^2 w_b}{\partial t^2} - \frac{D}{S}\left(\frac{\partial^2 w_b}{\partial x^2} + \frac{\partial^2 w_b}{\partial y^2}\right). \tag{11}$$

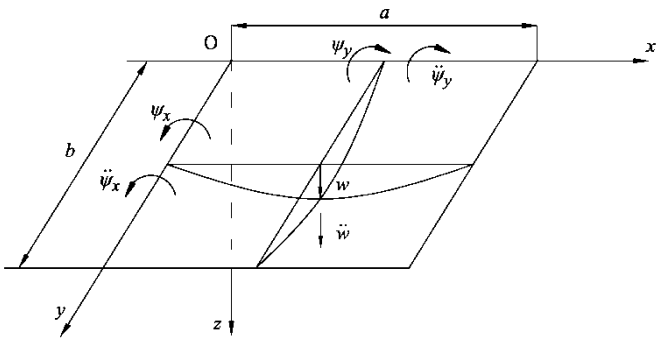

Figure 1: Displacements of rectangular plate

Analytical solutions for simply supported plates and plates with two opposite edges simply supported are presented in [4]. Rigorous solutions for complex boundary conditions can be obtained by employing the method of separation of variables, as shown in [10].

3 SHEAR LOCKING-FREE FINITE ELEMENT

Complete derivation of rectangular and triangular shear locking-free finite elements is presented in [12] and here theoretical background related to the former is reviewed. A general finite element with n nodes and three d.o.f. per node, i.e. deflection and rotations around the x and y axis, is considered. The ordinary procedure for determining stiffness and the mass matrix in the case of a thin plate is used [16]. Bending deflection as a potential function is assumed in a polynomial form with a number of unknown coefficients which corresponds to the total number of d.o.f. N=3n

$$w_b = \langle a \rangle \{P\}_b, \tag{12}$$

where $\langle a \rangle$ is a row vector with terms a_i, i=0,1,...N-1, and

$$\{P\}_b^T = \langle P \rangle_b = \langle 1, x, y, x^2, xy, y^2 \ldots \rangle. \tag{13}$$

Total static deflection can be expressed in the following form

$$w = \langle a \rangle \left(\{P\}_b - \frac{D}{S}\frac{\partial^2 \{P\}_b}{\partial x^2} - \frac{D}{S}\frac{\partial^2 \{P\}_b}{\partial y^2} \right). \tag{14}$$

Angles of rotation (9) yield

$$\psi_x = -\langle a \rangle \frac{\partial \{P\}_b}{\partial x}, \qquad \psi_y = -\langle a \rangle \frac{\partial \{P\}_b}{\partial y}. \tag{15}$$

By taking coordinate values x_l and y_l for each node, l=1,2...n , into account in Eqs. (14) and (15), the relation between the nodal displacements and the unknown coefficients a_i is obtained

$$\{\delta\} = [C]\{a\}, \tag{16}$$

where $[C]$ includes x_l and y_l and

$$\{\delta\}=\begin{Bmatrix}\{\delta\}_1\\ \vdots\\ \{\delta\}_n\end{Bmatrix},\qquad \{\delta\}_l=\begin{Bmatrix}w_l\\ \varphi_l\\ \psi_l\end{Bmatrix}. \tag{17}$$

Now, for the given nodal displacement vector $\{\delta\}$, the corresponding coefficient vector $\{a\}$ can be determined from (16)

$$\{a\}=[C]^{-1}\{\delta\}. \tag{18}$$

Substituting (18) into (12) yields

$$w_b=\langle\phi\rangle_b\{\delta\}, \tag{19}$$

where

$$\langle\phi\rangle_b=\langle P\rangle_b[C]^{-1} \tag{20}$$

is the vector of the bending shape functions. In a similar way, shear deflection can be presented in the form

$$w_s=\langle P\rangle_s\{a\}, \tag{21}$$

where according to (14)

$$\langle P\rangle_s=-\frac{D}{S}\frac{\partial^2\langle P\rangle_b}{\partial x^2}-\frac{D}{S}\frac{\partial^2\langle P\rangle_b}{\partial y^2}. \tag{22}$$

Substituting (54) into (57) yields

$$w_s=\langle\phi\rangle_s\{\delta\}, \tag{23}$$

where

$$\langle\phi\rangle_s=\langle P\rangle_s[C]^{-1} \tag{24}$$

is the vector of the shear shape functions.

Total deflection according to (8) reads

$$w=\langle\phi\rangle\{\delta\}, \tag{25}$$

where

$$\langle\phi\rangle=\langle\phi\rangle_b+\langle\phi\rangle_s \tag{26}$$

is the vector of the total shape functions. Columns of the inverted matrix $[C]$ are vectors of coefficients a_i obtained for the unit value of particular nodal displacements

$$[C]^{-1}=\left[\{A\}_1\{A\}_2\ldots\{A\}_N\right], \tag{27}$$

where

$$\{A\}_j^T=\langle A\rangle_j=\left\langle a_0^j\ a_1^j\ldots a_{N-1}^j\right\rangle. \tag{28}$$

Bending curvatures and warping are presented in the form

$$\{\kappa\}_b = -\begin{Bmatrix} \dfrac{\partial^2 w_b}{\partial x^2} \\ \dfrac{\partial^2 w_b}{\partial y^2} \\ 2\dfrac{\partial^2 w_b}{\partial x \partial y} \end{Bmatrix} \tag{29}$$

Substituting (19) with (20) into (29) yields

$$\{\kappa\}_b = -[L]_b \{\delta\}, \tag{30}$$

where

$$[L]_b = [H]_b [C]^{-1}, \qquad [H]_b = \begin{bmatrix} \dfrac{\partial^2 \langle P \rangle_b}{\partial x^2} \\ \dfrac{\partial^2 \langle P \rangle_b}{\partial y^2} \\ 2\dfrac{\partial^2 \langle P \rangle_b}{\partial x \partial y} \end{bmatrix}. \tag{31}$$

Now it is possible to determine the bending stiffness matrix by employing a general formulation from the finite element method based on the variational principle

$$[K]_b = \int_A [L]_b^T [D]_b [L]_b \, \mathrm{d}A, \tag{32}$$

where $[D]_b$ is the matrix of plate flexural rigidity. Furthermore, substituting (31) into (32) yields

$$[K]_b = [C]^{-T} [B] [C]^{-1}, \tag{33}$$

where symbolically $[C]^{-T} = \left([C]^{-1}\right)^T$ and

$$[B] = \int_A [H]_b^T [D]_b [H]_b \, \mathrm{d}A. \tag{34}$$

By taking (31) and (33) into account, (35) can be presented in the form

$$[B] = D\left([I]_1 + \nu\left([I]_2 + [I]_3\right) + [I]_4 + 2(1-\nu)[I]_5\right), \tag{35}$$

where

$$[I]_1 = \int_A \frac{\partial^2 \{P\}_b}{\partial x^2} \frac{\partial^2 \langle P \rangle_b}{\partial x^2} \mathrm{d}A, \tag{36}$$

$$[I]_2 = \int_A \frac{\partial^2 \{P\}_b}{\partial x^2} \frac{\partial^2 \langle P \rangle_b}{\partial y^2} \mathrm{d}A = [I]_3^T, \tag{37}$$

$$[I]_4 = \int_A \frac{\partial^2 \{P\}_b}{\partial y^2} \frac{\partial^2 \langle P \rangle_b}{\partial y^2} \mathrm{d}A, \tag{38}$$

$$[I]_5 = \int_A \frac{\partial^2 \{P\}_b}{\partial x \partial y} \frac{\partial^2 \langle P \rangle_b}{\partial x \partial y} \mathrm{d}A. \tag{39}$$

Similarly, one can write for the shear strain vector

$$\{\gamma\} = \begin{Bmatrix} \dfrac{\partial w_s}{\partial x} \\ \dfrac{\partial w_s}{\partial y} \end{Bmatrix}, \tag{40}$$

$$\{\gamma\} = [L]_s \{\delta\}, \tag{41}$$

where

$$[L]_s = [H]_s [C]^{-1}, \tag{42}$$

$$[H]_s = \begin{bmatrix} \dfrac{\partial \langle P \rangle_s}{\partial x} \\ \dfrac{\partial \langle P \rangle_s}{\partial y} \end{bmatrix}. \tag{43}$$

Analogously to (32), the shear stiffness matrix based on the variational principle is presented in the form

$$[K]_s = \int_A [L]_s^T [D]_s [L]_s \mathrm{d}A, \tag{44}$$

Where $[D]_s = S \begin{bmatrix} 1 & 0 \\ 0 & 1 \end{bmatrix}$. After some substitutions, according to [12], one can write

$$[K]_s = [C]^{-T} [S] [C]^{-1}, \tag{45}$$

$$[S] = S \int_A [H]_s^T [H]_s \mathrm{d}A, \tag{46}$$

$$[S] = S([I]_6 + [I]_7), \tag{47}$$

$$[I]_6 = \int_A \frac{\partial \{P\}_s}{\partial x} \frac{\partial \langle P \rangle_s}{\partial x} \mathrm{d}A, \tag{48}$$

$$[I]_7 = \int_A \frac{\partial \{P\}_s}{\partial y} \frac{\partial \langle P \rangle_s}{\partial y} \mathrm{d}A. \tag{49}$$

Hence, the complete stiffness matrix is

$$[K] = [K]_b + [K]_s = [C]^{-T} ([B] + [S]) [C]^{-1}. \tag{50}$$

According to the general formulation of the mass matrix in the finite element method based on the variational principle one can write

$$[M] = m\int_A \{\phi\}\langle\phi\rangle \mathrm{d}A, \tag{51}$$

where $\{\phi\}$ is the vector of the total shape functions (26). Taking (20) and (24) into account yields

$$[M] = m[C]^{-T}[I]_0[C]^{-1}, \tag{52}$$

Where $[I]_0 = \int_A \{P\}\langle P\rangle \mathrm{d}A$ and $\{P\} = \{P\}_b + \{P\}_s$, Eqs. (13) and (22).

4 NUMERICAL EXAMPLES – COMPARATIVE STUDY

Based on the above described theoretical background, an in-house code has been developed and applied to vibration analysis of square and rectangular plates, having different boundary conditions and different relative thicknesses. In all numerical examples values of Young's modulus is set at $2.1\cdot10^{11}$ N/m^2, material density yields 7850 kg/m^3, and the value of shear correction factor is set to 5/6. Results obtained by the developed code are denoted with PS (Present solution).

4.1 Simply supported plate, SSSS

Non-dimensional thickness parameters of simply supported square plate are presented in Table 1. They are compared with analytical solution, assumed mode method AMM [8] and NASTRAN values obtained by 2D and 3D FEM analysis [13]. Analytical results are rigorous since they also result from direct application of the Mindlin theory. The first 6 natural modes determined by 3D FEM NASTRAN analysis are shown in Figure 2 as relief map, where sagging and hogging modal areas are noticeable. FEM mesh used in 2D and 3D NASTRAN model is 8x8 and 8x8x4 elements, respectively. Boundary conditions for 3D FEM model are specified for nodes at the middle surface. In the considered case NASTRAN 2D and 3D frequency parameter values are very similar, and with PS values band the exact solution. The AMM values are very close to the analytical solution.

Table 1: Frequency parameter $\lambda = \omega a^2\sqrt{\rho h / D}/\pi^2$ of square plate, SSSS, h/a=0.2

MIN* *m,n*	Analytical [4]	AMM	PS	NASTRAN	
				2D	3D
1,1	1.768	1.768	1.803	1.682	1.651
1,2; 2,1	3.866	3.869	4.024	3.791	3.717
2,2	5.588	5.591	5.827	5.249	5.142
1,3; 3,1	6.601	6.601	7.072	6.478	6.436
2,3; 3,2	7.974	7.975	8.466	7.336	7.273
3,3	9.980	9.827	10.519	8.560	8.657

*MIN - mode identification number

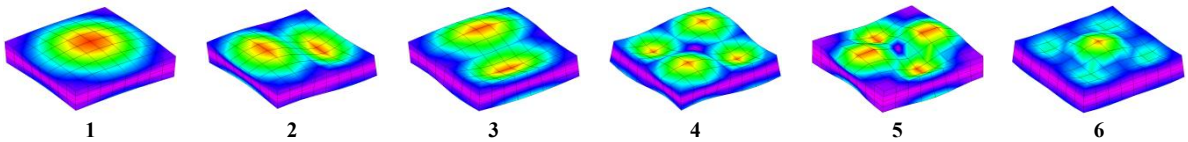

Figure 2: Natural modes of a simply supported square plate, 3D FE analysis

4.2 Clamped square plate, CCCC

Vibration analysis of clamped plate is done by FEM using mesh of 8 x 8 elements. AMM, PS results and NASTRAN 2D and 3D results are listed in Table 2. In 3D FEM model all boundary nodes are fixed. The obtained results are compared with those from [5], which are obtained by the Rayleigh-Ritz method and due to high accuracy can be used for evaluation of the present solutions. AMM, as a variant of Rayleigh-Ritz method gives actually nearly the same results. As in the case of simply supported plate, PS and NASTRAN results band the referent values and discrepancies are of the same order of magnitude. The flexural natural modes of a clamped square plate determined by AMM and 2D FEM NASTRAN are shown in Fig. 3, and those determined by 3D FEM NASTRAN analysis are presented in Fig. 4.

Table 2: Frequency parameter $\lambda = \omega a^2 \sqrt{\rho h / D} / \pi^2$ of square plate, CCCC, h/a=0.2

Mode no.	Liew et al. [5]	AMM	PS	NASTRAN	
				2D	3D
1	2.687	2.688	2.724	2.657	2.758
2	4.691	4.691	4.842	4.607	4.787
3	4.691	4.691	4.842	4.607	4.787
4	6.298	6.299	6.527	5.956	6.164
5	7.177	7.177	7.640	6.942	7.240
6	7.276	7.276	7.697	7.013	7.357

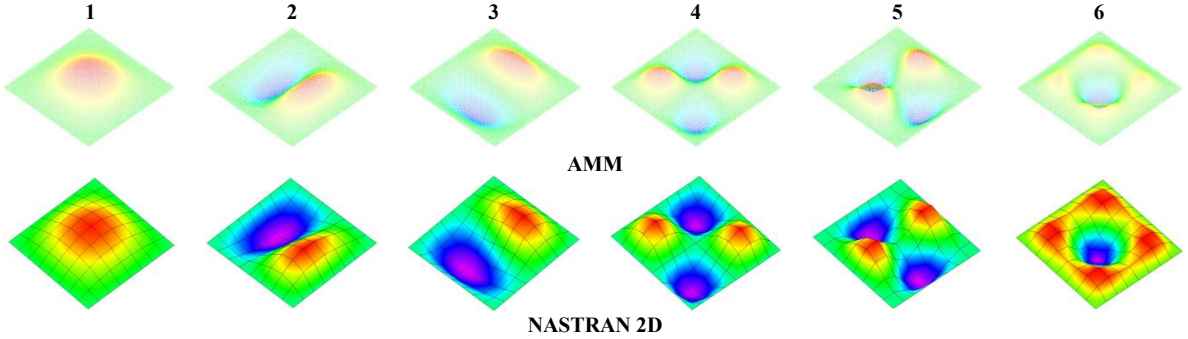

Figure 3: Natural modes of a clamped square plate, AMM and NASTRAN 2D analysis

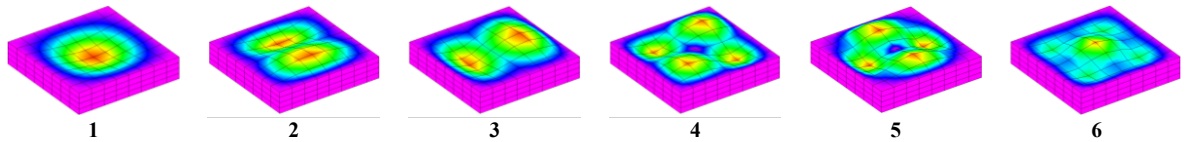

Figure 4: Natural modes of a clamped square plate, 3D FE analysis

4.3 Vibrations of rectangular plates

Further, rectangular plates with different combinations of boundary conditions and various relative thicknesses and length to width ratios are analysed. Values of non-dimensional frequencies parameters for SCCC, SCCS and FSSC boundary conditions are presented in Tables, 3, 4 and 5, respectively. Comparisons with the results available in the relevant literature are also provided and similar comments as for square plates are valid. For illustration natural modes for SCCC and FSSC boundary conditions are shown in Figs. 5 and 6, respectively.

Table 3: Frequency parameter $\lambda = \omega b^2 \sqrt{\rho h / D}$ of rectangular plate, SCCC, a/b=0.6

h/b	METHOD	1	2	3	4
0.001	Xing & Liu [17]	7.024	9.666	14.608	18.203
	Liew et al. [5]	7.060	9.731	14.663	18.217
	AMM	7.061	9.729	14.663	18.218
	PS	6.966	9.432	14.173	17.981
	NASTRAN 2D	6.930	9.331	14.196	17.955
0.1	Xing & Liu [17]	5.787	7.709	11.168	12.919
	Liew et al. [5]	5.862	7.873	11.342	12.982
	AMM	5.862	7.873	11.342	13.071
	PS	5.851	7.823	11.480	13.252
	NASTRAN 2D	5.775	7.534	10.706	12.825
0.2	Xing & Liu [17]	4.154	5.472	7.725	8.293
	Liew et al. [5]	4.282	5.687	7.900	8.373
	AMM	4.282	5.687	7.900	8.373
	PS	4.323	5.796	8.269	8.735
	NASTRAN 2D	4.247	5.535	7.528	8.319

Table 4: Frequency parameter $\lambda = \omega b^2 \sqrt{\rho h / D}$ of rectangular plate, SCCS, a/b=0.6

h/b	METHOD	1	2	3	4
0.001	Xing & Liu [17]	5.319	8.449	13.756	15.014
	Liew et al. [5]	5.341	8.479	13.779	15.049
	AMM	5.341	8.481	13.780	15.049
	PS	5.275	8.278	13.440	14.853
	NASTRAN 2D	5.234	8.153	13.329	14.789
0.1	Xing & Liu [17]	4.674	7.092	10.861	11.602
	Liew et al. [5]	4.716	7.171	10.948	11.640
	AMM	4.730	7.181	10.954	11.674
	PS	4.692	7.129	11.109	11.877
	NASTRAN 2D	4.602	6.814	10.330	11.520
0.2	Xing & Liu [17]	3.640	5.281	7.664	7.972
	Liew et al. [5]	3.712	5.397	7.764	8.025
	AMM	3.712	5.397	7.764	8.025
	PS	3.746	5.499	8.130	8.353
	NASTRAN 2D	3.659	5.209	7.377	7.973

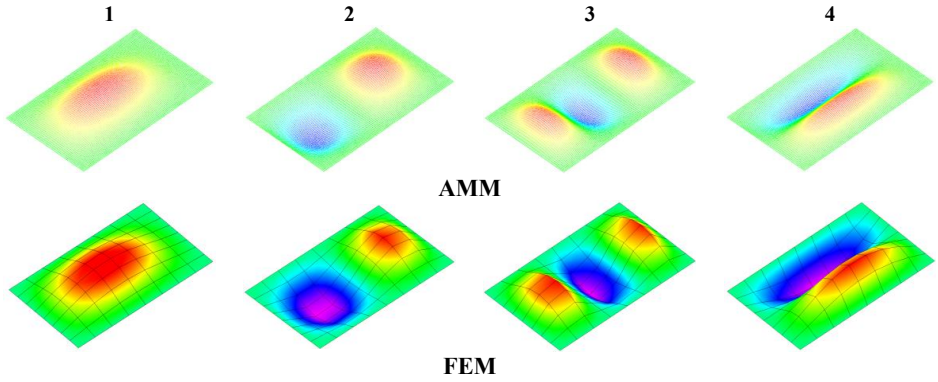

Figure 5: Mode shapes of rectangular plate, a/b=0.6, SCCC, AMM and NASTRAN 2D analysis

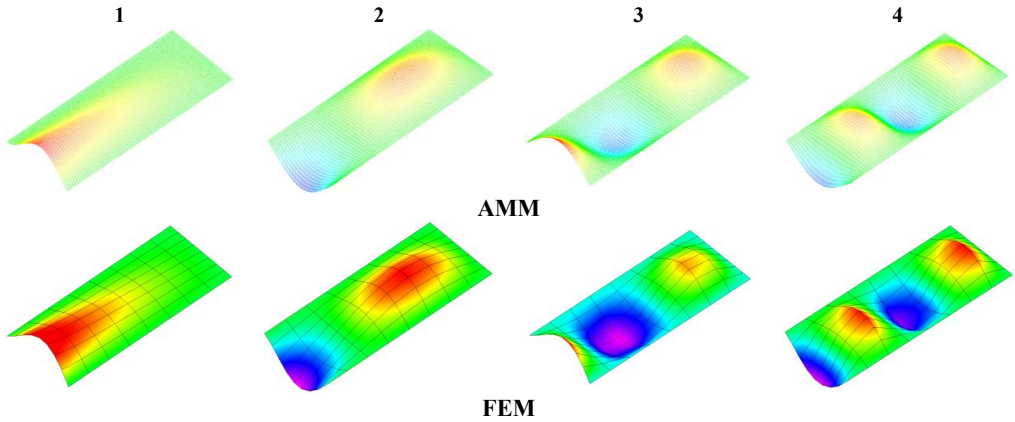

Figure 6: Mode shapes of rectangular plate, a/b=0.4, FSSC, AMM and NASTRAN 2D analysis

Table 5: Frequency parameter $\lambda = \omega b^2 \sqrt{\rho h / D}$ of rectangular plate, FSSC, a/b=0.4

h/b	METHOD	1	2	3	4
0.001	Liew et al. [5]	9.874	11.346	14.900	19.539
	AMM	9.872	11.403	14.944	20.317
	PS	9.896	11.172	14.017	18.746
	NASTRAN 2D	9.823	10.945	13.363	17.404
0.1	Liew et al. [5]	7.941	8.970	11.135	14.462
	AMM	8.055	9.068	11.206	14.508
	PS	8.099	8.965	11.001	14.476
	NASTRAN 2D	7.985	8.635	10.196	12.825
0.2	Liew et al. [5]	5.594	6.305	7.752	9.828
	AMM	5.594	6.305	7.752	9.828
	PS	5.765	6.386	7.885	10.325
	NASTRAN 2D	5.669	6.126	7.277	8.993

4.4 Convergence study

The convergence of the proposed finite element formulation is demonstrated in the case of a

simply supported square plate. Natural frequencies are determined by the finite element model for three mesh densities, i.e. 6x6=36, 8x8=64 and 10x10=100 elements, and three values of a thickness ratio h/a: 0.001, 0.1 and 0.2. The obtained frequency parameters are listed in Table 6 and compared with the exact analytical solution as well as with the NASTRAN and Abaqus results, [13,14]. In order to have better insight into the convergence, frequency parameter for the 1st, 4th and 7th modes are shown in Fig. 7. For thin plate (h/a=0.001), the present solution converges to the exact value, faster than the NASTRAN and Abaqus results, which converge from the opposite sides. PS values for moderately thick plate (h/a=0.1) are very close to the exact values for all three mesh densities, while the NASTRAN and Abaqus results converge to a lower value than the exact solution. The discrepancy is reduced for higher modes. In the case of thick plate (h/a=0.2), the variation of the PS values, which are somewhat higher than the exact solution, is rather small. The NASTRAN and Abaqus results show the same tendency as in the previous case.

Table 6: Convergence of frequency parameter $\lambda = \omega a^2 \sqrt{\rho h / D}$ of square plate, SSSS

h/a	METHOD	1 /11/*	2 /12/	3 /21/	4 /22/	5 /13/	6 /31/	7 /23/	8 /32/
0.001	Senjanović et al. [4]	19.739	49.348	49.348	78.956	98.694	98.694	128.302	128.302
	PS (6x6)	19.459	48.326	48.326	75.103	96.867	96.867	120.658	120.658
	PS (8x8)	19.592	48.744	48.744	76.603	98.487	98.487	123.374	123.374
	PS (10x10)	19.629	48.944	48.944	77.384	97.859	97.859	124.933	124.933
	NASTRAN (6x6)	19.150	47.343	47.343	71.762	95.014	95.084	115.491	115.491
	NASTRAN (8x8)	19.377	48.115	48.115	74.420	96.381	96.381	119.255	119.255
	NASTRAN (10x10)	19.488	48.497	48.497	75.803	97.063	97.063	122.044	122.044
	Abaqus (6x6)	20.205	54.743	54.743	86.623	132.223	132.223	158.355	158.355
	Abaqus (8x8)	20.000	52.251	52.251	83.203	115.389	115.389	143.839	143.839
	Abaqus (10x10)	19.906	51.169	51.169	81.652	124.895	124.895	137.892	137.892
0.1	Senjanović et al. [4]	19.065	45.483	45.483	69.794	85.038	85.038	106.684	106.684
	PS (6x6)	18.959	45.581	45.581	69.055	87.636	87.636	107.334	107.334
	PS (8x8)	19.063	45.821	45.821	69.908	87.320	87.320	108.019	108.019
	PS (10x10)	19.117	45.949	45.949	70.374	87.230	87.230	108.520	108.520
	NASTRAN (6x6)	18.022	42.985	42.985	60.972	80.069	80.090	89.787	89.787
	NASTRAN (8x8)	18.243	43.927	43.927	64.251	82.692	82.750	96.541	96.541
	NASTRAN (10x10)	18.339	44.380	44.380	65.918	83.926	84.008	100.115	100.115
	Abaqus (6x6)	18.906	49.078	49.078	73.469	106.435	106.605	122.766	122.766
	Abaqus (8x8)	18.663	46.971	46.971	70.836	95.661	95.831	114.072	114.072
	Abaqus (10x10)	18.544	46.037	46.037	69.609	91.190	91.354	110.279	110.279
0.2	Senjanović et al. [4]	17.449	38.152	38.152	55.150	65.145	65.145	78.697	78.697
	PS (6x6)	17.662	39.476	39.476	56.997	70.314	70.314	83.630	83.630
	PS (8x8)	17.733	39.454	39.454	57.016	69.123	69.123	82.667	82.667
	PS (10x10)	17.767	39.451	39.451	57.081	68.584	68.584	82.280	82.280
	NASTRAN (6x6)	16.348	36.264	36.264	48.588	60.567	60.641	65.908	65.908
	NASTRAN (8x8)	16.535	37.148	37.148	51.336	63.253	63.383	71.578	71.578
	NASTRAN (10x10)	16.617	37.562	37.562	52.679	64.503	64.667	74.427	74.427
	Abaqus (6x6)	16.796	40.014	40.014	56.260	76.247	76.591	85.787	85.787
	Abaqus (8x8)	16.610	38.620	38.620	54.749	70.632	70.966	81.596	81.596
	Abaqus (10x10)	16.523	37.997	37.997	54.046	68.169	68.493	79.675	79.675

*/*m,n*/ - mode identification number, *m* and *n* number of half waves in *x* and *y* direction

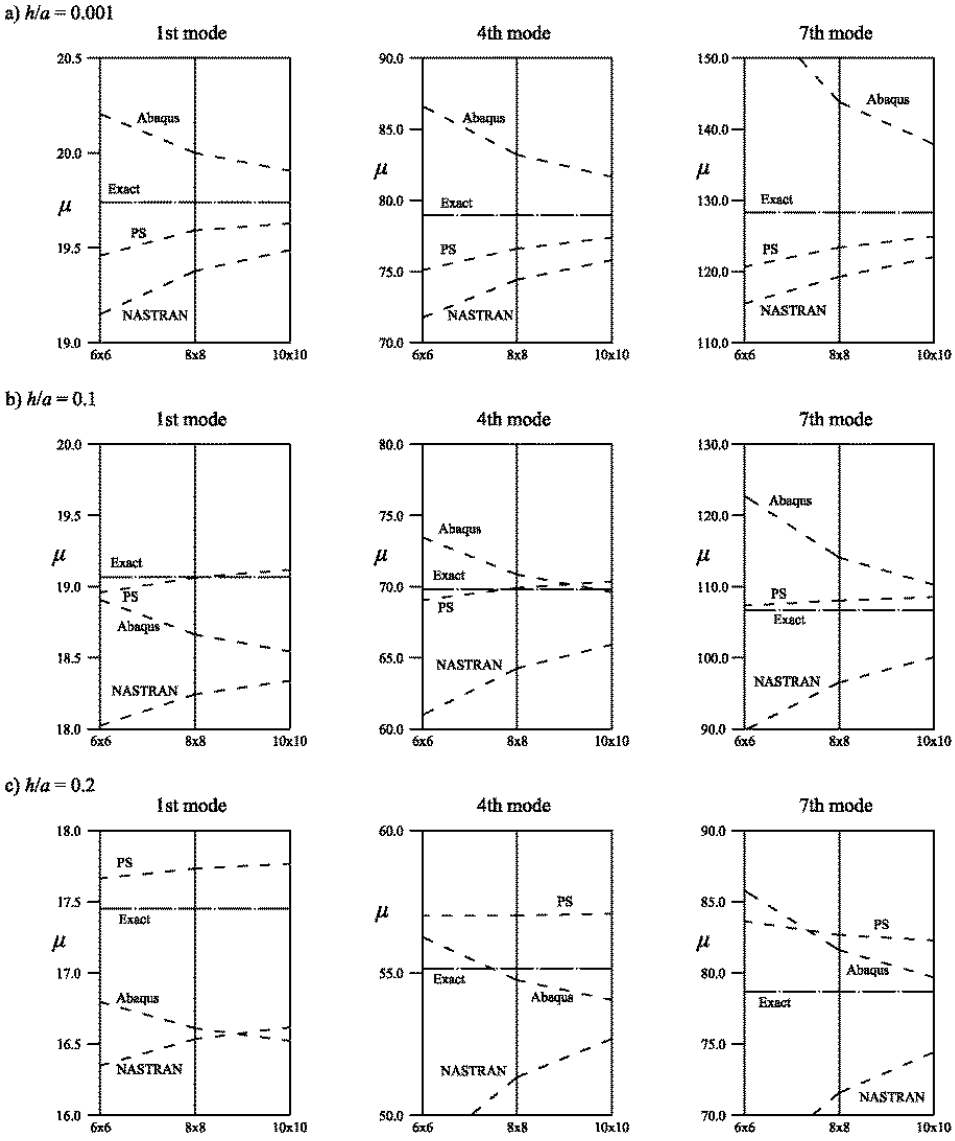

Figure 7: Convergence of frequency parameter $\lambda = \omega a^2 \sqrt{\rho h / D}$ of simply supported square plate

5 CONCLUDING REMARKS

Newly developed shear locking-free finite element for vibration analysis of moderately thick plate is presented and validated with in extensive numerical calculations. The results are compared to recently published analytical solutions, assumed mode method, Rayleigh-Ritz solutions and some general commercial FE software results. Decomposition of total deflection into bending and shear components and reduction of three differential equations into one single

with bending deflection as a potential function, provides clear physical insight into the problem. Moreover, when the FE is derived using the proposed procedure based on the advanced theory of thick plate vibrations, shear locking phenomenon doesn't appear. Therefore usual procedure for shear locking elimination are not required in this case.

ACKNOWLEDGEMENTS

This work was supported by a National Research Foundation of Korea (NRF) grant funded by the Korean Government (MSIP) through GCRC-SOP (Grant No. 2011-0030013).

REFERENCES

1 E. Reissner, "The effect of transverse shear deformation on the bending of elastic plate", *Trans. ASME J. Appl. Mech.*, 12, A69-A77 (1945).
2 R.D. Mindlin, "Influence of rotary inertia and shear on flexural motions of isotropic elastic plates", *J. Appl. Mech.*, 18, 31-38 (1951).
3 K.M. Liew, Y. Xiang, A. Kitipornchai, "Research on thick plate vibration: a literature survey", *J. Sound Vib.*, 180, 163-176 (1995).
4 I. Senjanović, N. Vladimir, M. Tomić, "An advanced theory of moderately thick plate vibrations", *J. Sound Vib.*, 332, 1868-1880 (2013).
5 K.M. Liew, Y. Xiang, S. Kitipornchai, "Transverse vibration of thick plates – I. Comprehensive sets of boundary conditions", *Comput. Struct.*, 49, 1-29 (1993).
6 D.J. Dawe, O.L. Roufaeil, "Rayleigh-Ritz vibration analysis of Mindlin plates", *J. Sound Vib.*, 69, 345-359 (1980).
7 Y.K. Cheung, D. Zhou, "Vibrations of moderately thick plates in terms of a set of static Timoshenko beam functions", *Comput. Struct.*, 78, 757-768 (2000).
8 K.H. Kim, B.H, Kim, T.M. Choi, D.S. Cho, "Free vibration analysis of rectangular plate with arbitrary edge constraints using characteristic orthogonal polynomials in assumed mode method", *Int. J. Nav. Arch. Ocean Engng.*, 4, 267-280 (2012).
9 D.S. Cho, N. Vladimir, T.M. Choi, "Approximate natural vibration analysis of rectangular plates with openings using assumed mode method", *Int. J. Nav. Arch. Ocean Engng.*, 5, 478-491 (2013).
10 I. Senjanović, M. Tomić, N. Vladimir, D.S. Cho, "Analytical solution for free vibrations of a moderately thick rectangular plate", *Math. Probl. Engng.*, 5, 478-491 (2013).
11 I. Senjanović, N. Vladimir, N. Hadžić, "Modified Mindlin plate theory and shear locking-free finite element formulation", *Mech. Res. Comm.*, 55, 95-104 (2014).
12 I. Senjanović, N. Vladimir, D.S. Cho, "A new finite element formulation for vibration analysis of thick plates", *Int. J. Nav. Arch. Ocean Engng.*, 2014. (accepted for publication).
13 MSC Software, *MD Nastran 2010 Dynamic analysis user's guide*, (2010).
14 Assault Systémes, *Abaqus Analysis User's Manual*, Version 6.8 (2008).
15 I. Senjanović, N. Vladimir, "Physical insight into Timoshenko beam theory and its modification with extension", *Struct. Engng. Mech.,* 48, 519-545 (2013).
16 R. Szilard, "*Theories and applications of Plate Analysis*", John Wiley & Sons, 2004.
17 Y. Xing, B. Liu, "Characteristic equations and closed-form solution for free vibrations of rectangular Mindlin plates", *Acta Mech. Solida Sinica*, 22(2), 125-136 (2009).